Journal of Molecular Catalysis A: Chemical 326 (2010) 99–106

Contents lists available at ScienceDirect

Journal of Molecular Catalysis A: Chemical

journal homepage: www.elsevier.com/locate/molcata

Synthesis, characterization and catalytic activity of trimetallic nanoparticles in the Suzuki C–C coupling reaction

P. Venkatesan, J. Santhanalakshmi*

Department of Physical Chemistry, University of Madras, Guindy Campus, Chennai 600 025, Tamil Nadu, India

ARTICLE INFO

Article history:
Received 9 December 2009
Received in revised form 21 April 2010
Accepted 23 April 2010
Available online 21 May 2010

Keywords:
Trimetallic nano catalysis
HPLC study
CTAB capping agent
Pdnp nanocatalysts
Suzuki reaction

ABSTRACT

Pd containing trimetallic nanoparticles (Pdtnp) are synthesized using chemical method with cetyltrimethylammonium bromide (CTAB) as the capping agent. The particle sizes are characterized by HRTEM, and XRD measurements. The catalytic activities of Pdtnp are tested using Suzuki C–C coupling reaction. The product yield, reaction time and recyclability of the recovered catalysts are studied. The effects of solvent medium, nature of base and the reaction temperature for Pdtnp catalysts are optimized. Pdtnp exhibited better Suzuki reaction catalysis than Pdnp.

1. Introduction

Metallic nanoparticles of definite size are synthesized via a "bottoms-up" approach and surface modified with special functional groups. The nanoscale particles are generally motivated by the change in physical and chemical properties as compared to bulk materials [1,2]. They are expected to be useful in various ways, like as catalysts [3–7], magnetic materials [8–11], semiconductors [12], electro-optic materials [13], drug delivery materials [14] and so on, and thus should be attractive to many researchers. The large surface-to-volume ratio of metallic nanoparticles makes them very attractive to use as catalysts for chemical reactions compared to other bulk catalytic materials [15]. This attractive property of metallic nanoparticles results in the surface atoms being very active. The surface atoms are so active that they result in changes in the size or shape of the nanoparticles during their catalytic function.

In the core–shell-structured bimetallic nanoparticles thus prepared, the catalytic activity of shell atoms can be electronically affected by the core atoms [16]. Based on the concept of electronic effect in bimetallic nanoparticles having a core–shell structure, a "triple core–shell structure," in which one element form a core, the second element covers the core, forming an interlayer, and the third element covers the interlayer, forming a shell, has been proposed. A successive electronic effect is expected in this triple core–shell-structured trimetallic nanoparticle. However, only few reports have been published on trimetallic nanoparticles having a triple core–shell structure [17–20].

Recent studies indicate that Palladium based nanostructures are also attractive for a number of catalytic applications and have been demonstrated in a variety of reactions that include Heck coupling [21–24], Suzuki coupling [25–28] and hydrogenation [29,30], etc. In particular, bimetallic systems have been shown to exhibit enhanced catalytic activity for multiple reactions including the C–C coupling reaction [31–35], and previously reported the present of Au–Ag–Pd trimetallic nanoparticles, as well as their catalytic activities towards Heck C–C coupling reaction [36]. Interestingly, the catalytic activity strongly depended on the composition. Only the trimetallic nanoparticles with strictly designed composition had very high activity, which suggests that the triple core–shell structure was spontaneously produced at the specific composition.

In the present work, the synthesis of trimetallic nanoparticles having an Au-core structure by a combination of the preparation of bimetallic nanoparticles by co-reduction with the formation of core/shell-structured bimetallic nanoparticles by self-organization in physical mixture. The formation of trimetallic nanoparticles has been characterized by UV–vis spectral change, HRTEM images, FT-IR spectra, XRD spectra, SEM-EDX and catalytic studies. The catalytic Suzuki reaction between phenylboronic acid and iodobenzene in aqueous solution is investigated in order to provide a mechanistic understanding of surface atoms in the catalysis of this reaction. The catalytic activity of trimetallic nanoparticles was higher than the corresponding mono- and bimetallic nanoparticles. This high catalytic activity can be understood by sequential elec-

* Corresponding author. Tel.: +91 44 22202816.
E-mail addresses: venkatesanorg@gmail.com (P. Venkatesan), jslakshmi@yahoo.co.in (J. Santhanalakshmi).

1381-1169/$ – see front matter © 2010 Elsevier B.V. All rights reserved.
doi:10.1016/j.molcata.2010.04.015

tronic charge transfer from surface Pd atoms to interlayered Ag atoms and then to core Au atoms.

2. Experimental

2.1. Materials

Hydro tetrachloroauric acid ($HAuCl_4$) and silver nitrate ($AgNO_3$), Palladium Chloride ($PdCl_2$) from Ranbaxy Lab. Ltd. India, cetyltrimethylammonium bromide (CTAB), sodium borohydride ($NaBH_4$), ethanol, aryl halides and phenylboronic acids from Aldrich Chemicals with 99% purity are used as such. IR grade KBr was supplied by Sigma. Triple distilled water was used for making solutions.

2.2. Preparation of trimetallic nanoparticles

The colloidal dispersions of surfactant (CTAB)-protected Au–Ag bimetallic nanoparticles were prepared by refluxing of the aqueous solution of $HAuCl_4$ and $AgNO_3$ in the presence of CTAB [37]. The molar ratio of Au–Ag was 1/1, and the molar ratio of monomer unit of CTAB against total metal (R) was kept 40 in the present experiments. The colloidal dispersions of Pd nanoparticles are separately prepared by refluxing a H_2O/EtOH (1/1, v/v) solution of $PdCl_2$ in the presence of CTAB [38]. The colloidal dispersion of CTAB-protected Au–Ag (1/1) nanoparticle and that of CTAB-protected Pd nanoparticles are mixed at room temperature in the designated ratio. The mixed dispersions are kept stirring at least for a 24 h at room temperature to complete the self-organization reaction.

2.3. Size characterizations

The TEM photograph was taken on a JEOL model 1200 EX instrument operated in the accelerating voltage of 120 KV using Formvar coated copper grid. Powder X-ray analysis was carried out using a Philips PW 1050/37 model diffractometer, operating at 40 kV and 30 mA. Cu Kα radiation with a wavelength of 1.54 Å and a step size of 0.02° in the 2θ range, 30–80° was used. SEM-EDX experiments were carried out on a Hitachi S-3400 N instrument with EDX analyzer facility at 25 °C. The samples are prepared by placing a drop of the colloidal metal solution on a carbon coated copper grid and allowing the solvent to evaporate. Shimadzu UV-1601 double beam spectrometer using quartz cuvettes with 1 cm path-length was used for UV–vis spectra and FT-IR spectra are recorded using Bruker Tensor 27 instrument in KBr pellet at 25 °C.

2.4. Trimetallic nanoparticles (Pdtnp) catalyzed Suzuki coupling reaction

The reaction mixture consisting of 0.49 g of sodium acetate (0.49 g, 3 mmol), Phenylboronic acid (0.128 g, 1.05 mmol) and Iodobenzene (0.2 g, 1 mmol) and 150 ml of DMF–water (3:1, v/v) solvent are preheated to 100 °C for 2 min with stirring and in N_2 atm, immediately followed by the addition of trimetallic nanoparticles solution containing 0.1–0.5 mol% colloidal concentrations was added and continued the refluxing for 12 h. An aliquot amount of reaction mixture was taken every 3 min and cooled to room temperature the sample analysis was performed with a high-performance liquid chromatograph (HPLC, Hitachi-4500), equipped with a L4500A diode array detector (monitored wavelength at 254 nm).

3. Results and discussion

3.1. UV–visible spectroscopy (UV–vis)

The completion of formation reactions of monometallic palladium, bimetallic Au–Ag and trimetallic Au–Ag–Pd nanoparticles were followed by UV–visible spectroscopy as a function of time.

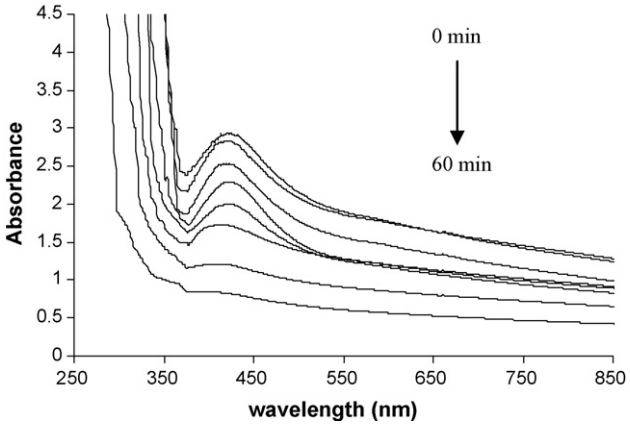

Fig. 1. UV–vis absorption spectra of CTAB stablized monometallic palladium nanoparticles (Pdnp) solution at different time interval in aqueous medium at 25 °C.

Fig. 1 shows the UV–vis spectral changes during the formation of monometallic Pd nanoparticles, the absence of peaks at 440 and 325 nm characteristic of unreduced Pd^{2+} indicates complete reduction of the metal ions. The metal ion binds well with CTAB micelle which was added to it. To the metal salt and the micelle system, few drops of $NaBH_4$ are added leading to the formation of metal nanoparticles. A peak at 325 and 440 nm due to the ligand-to-metal charge transfer transition of the $[PdCl_4]^{2-}$ ions disappears after heating a mixture of H_2PdCl_4 and CTAB in water—5% EtOH for 1 h, indicating that $[PdCl_4]^{2-}$ ions are completely reduced to element metal in the solution. The absorption in the visible region due to the band structure of metal nanoparticles increases, indicating that the Pd nanoparticles are formed. The Pd nanoparticle shows a sharp absorbance peak cannot be observed over the entire range due to the brown colour of the solution. The absorbance behaviour of the metal nanoparticle dispersions is found to be different from that of the metal salt solution.

In Fig. 2 the colloidal mixtures exhibited two prominent absorbance maxima at 428 and 545 nm. Both absorption bands are attributed to the characteristic Ag (428 nm) and Au (545 nm) spr bands. Note that Pd colloids do not have a distinct visible absorbance. The absorption spectra of the mixtures changed as the duration time was increased, the spr bands moved closer to

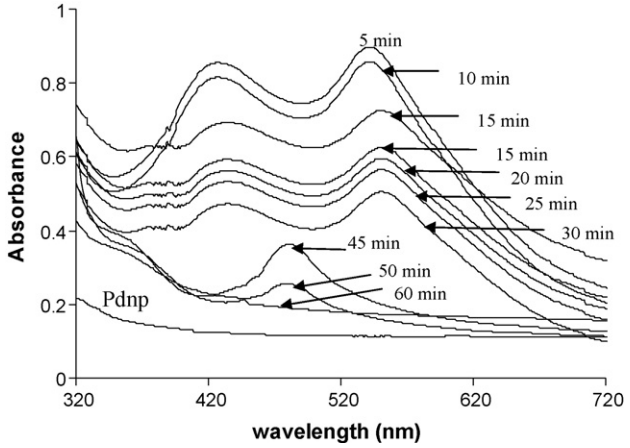

Fig. 2. UV–vis absorption spectra of CTAB stabilized trimetallic Au–Ag–Pd colloidal nanoparticles at different time intervals intermediates sample, the molar ratio of the surfactant to metal salts 100:0.5, respectively, in aqueous medium at 25 °C.

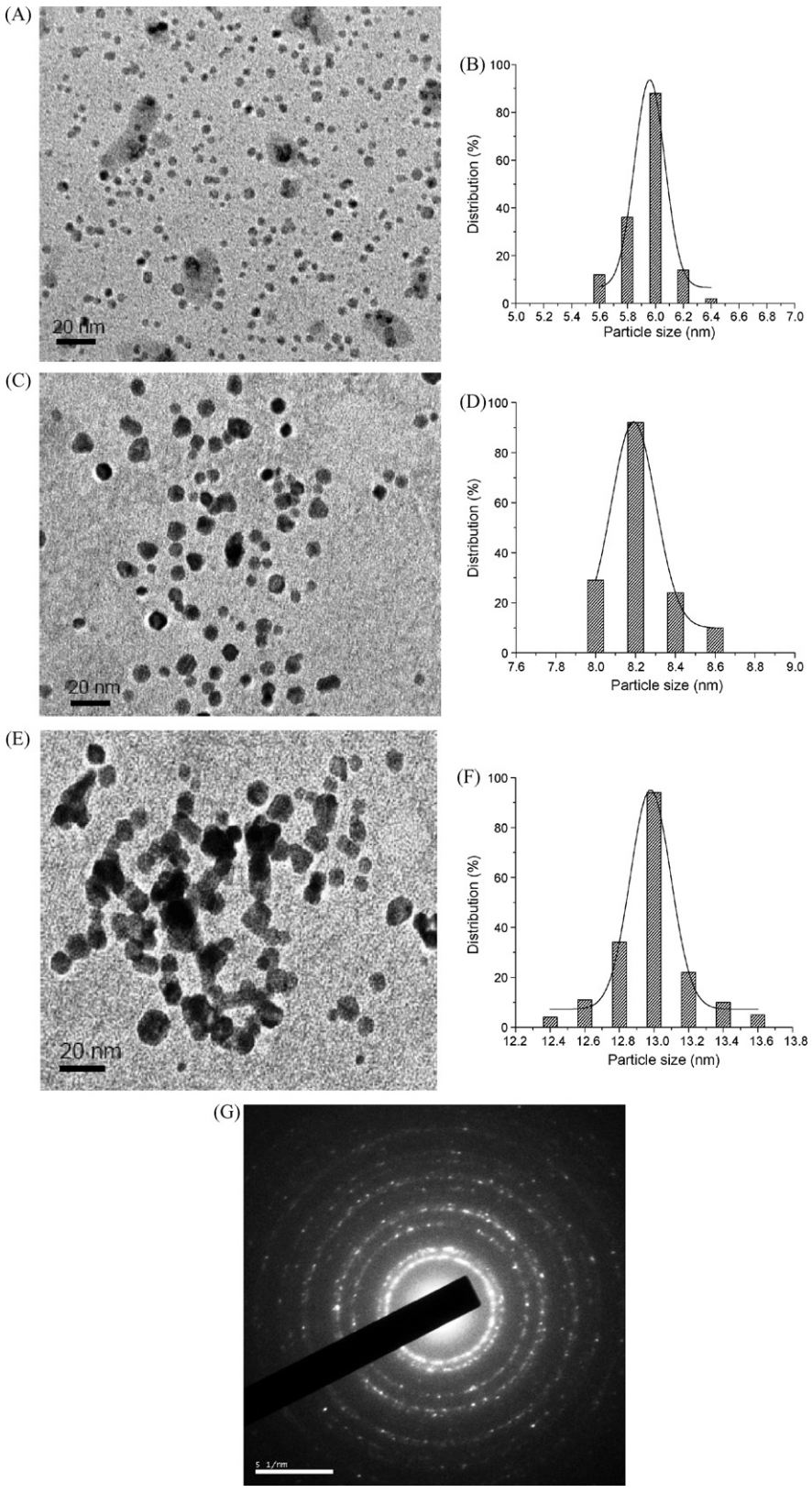

Fig. 3. Transmission electron microphotographs (HRTEM) picture of the CTAB stabilized (A) monometallic Pdnp, (C) bimetallic Au–Ag and (E) trimetallic Au–Ag–Pd colloidal nanoparticles solution. HRTEM image, bar indicates 10 nm, (B, D and F) particle size distribution and (G) electron diffraction pattern of tnp spectra in aqueous medium at 25 °C.

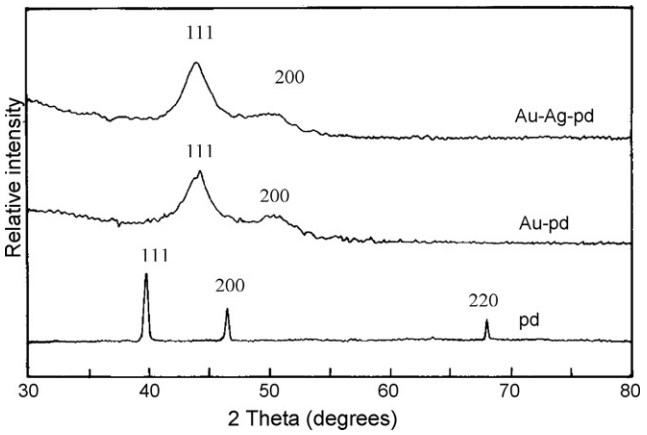

Fig. 4. X-ray diffraction (XRD) spectra of the CTAB stabilized mono-, bi- and trimetallic colloidal nanoparticles at 25 °C.

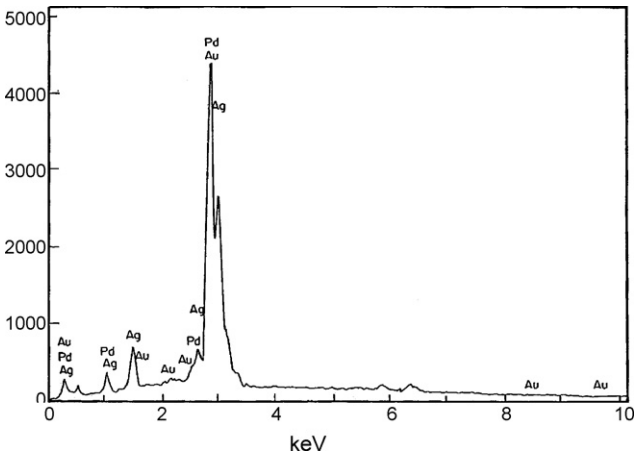

Fig. 5. Scanning electron microscopy EDX spectra of CTAB stabilized trimetallic Au–Ag–Pd nanoparticles at 25 °C.

one another and merged into a single peak over the course of the time intervals. The bimetallic Au–Ag nanoparticles as conformed after 45 min, further increased the time duration resulted in a continuous decrease in the absorption band until, eventually, no absorption peak was apparent after 60 min exposure. As the duration of the time was increased up to 24 h (overnight), there is no distinct change occurred in the shape or magnitude of the absorbance. Finally the color of the colloidal nanoparticles is dark brown.

Successive reduction strategies are an effective method to prepare core–shell structure bi and multi-metallic nanoparticles. One of the metal salts is reduced first to form the core, and then a second metal is deposited on the surface of pre-formed monometallic nanoparticles to form the shell. The formation of bi and multi-metallic core–shell nanoparticles dispersions depends on the kinetic and thermodynamics of the reduction of individual components. The complete reduction of Au (III), Ag (I), and Pd (II) metals requires 3, 5, and 10 min, respectively, as reported [39–41].

3.2. Transmission electron microscopy (HRTEM)

TEM images of typical CTAB stabilized monometallic palladium, bimetallic Au–Ag and trimetallic Au–Ag–Pd nanoparticles and their corresponding size distribution histograms are shown in Fig. 3(A, C and E). The images show that all three colloidal nanoparticles are well distributed and have 'near monodisperse' size distributions. The histogram of the particle sizes distribution is shown in Fig. 3(B, D and F) and Fig. 3G shows the electron diffraction pattern of tnp spectra. The uniform distribution of these particles combined with their small size leads to a good catalyst formation as exemplified in the use of these materials for the catalysis of organic reaction.

3.3. X- ray diffraction measurements (XRD)

Powder XRD analysis has been carried out to ascertain the nature of metallic particles. The diffractograms are carried out using dried powder. The XRD patterns showed that the metallic particles are crystalline in nature. The observed reflection positions correspond to (1 1 1) and (2 0 0) surfaces for different metal combinations as given in Fig. 4. The reflections of the trimetallic nanoparticles are different from the mono- and bimetallic components. The comparison of particle size between TEM and XRD data, the values obtained by XRD are slightly larger than the particle size deduced from TEM images.

3.4. Scanning electron microscopy (SEM-EDX)

Elemental mapping by EDX for a single particle of metallic nanoparticles revealed indeed that surfactants are present on the metal clusters. EDX analysis was done on several nanoparticles and obtained same results. EDX analysis results for Au–Ag–Pd trimetallic clusters (1:1:1) have been given in Fig. 5. This result showed the presence of all the three elements of metal nanoparticles.

3.5. Fourier transform infrared spectroscopy (FT-IR)

The FT-IR spectra of the CTAB, Pdnp and Pd containing tnp (Au–Ag–Pd, 1:1:1) prepared with CTAB as the capping agent and different mole ratios of trimetallic clusters, are presented in Fig. 6. In the spectral region 3550–2500 cm^{-1}, the C–H symmetric and antisymmetric stretching vibration frequency bands at 2850 and 2920 cm^{-1} seen for pure CTAB appear at 2862 and 2940 cm^{-1} for Pdnp–CTAB while at 2872 and 2958 cm^{-1} for Pdtnp–CTAB nanoparticles, respectively. The doublet at 1462 and 1472 cm^{-1} for pure CTAB may be attributed to the CH_2-scissoring mode of vibration, which are broad with lesser intensity and are shifted to lower wave numbers. These data clearly indicate that the binding of CTAB to Pd-shell in Pdtnp is analogous to the CTAB binding on to monometallic Pdnp. This ensures the presence of Pd in the shell region of tnp,

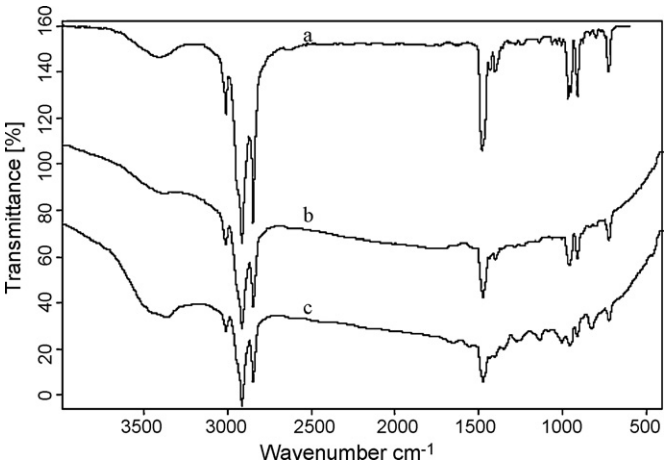

Fig. 6. FT-IR spectra of (a) cetyltrimethylammonium bromide (CTAB), (b) palladium nanoparticles (Pdnp) and (c) trimetallic nanoparticles (tnp), in KBr pellet at 25 °C.

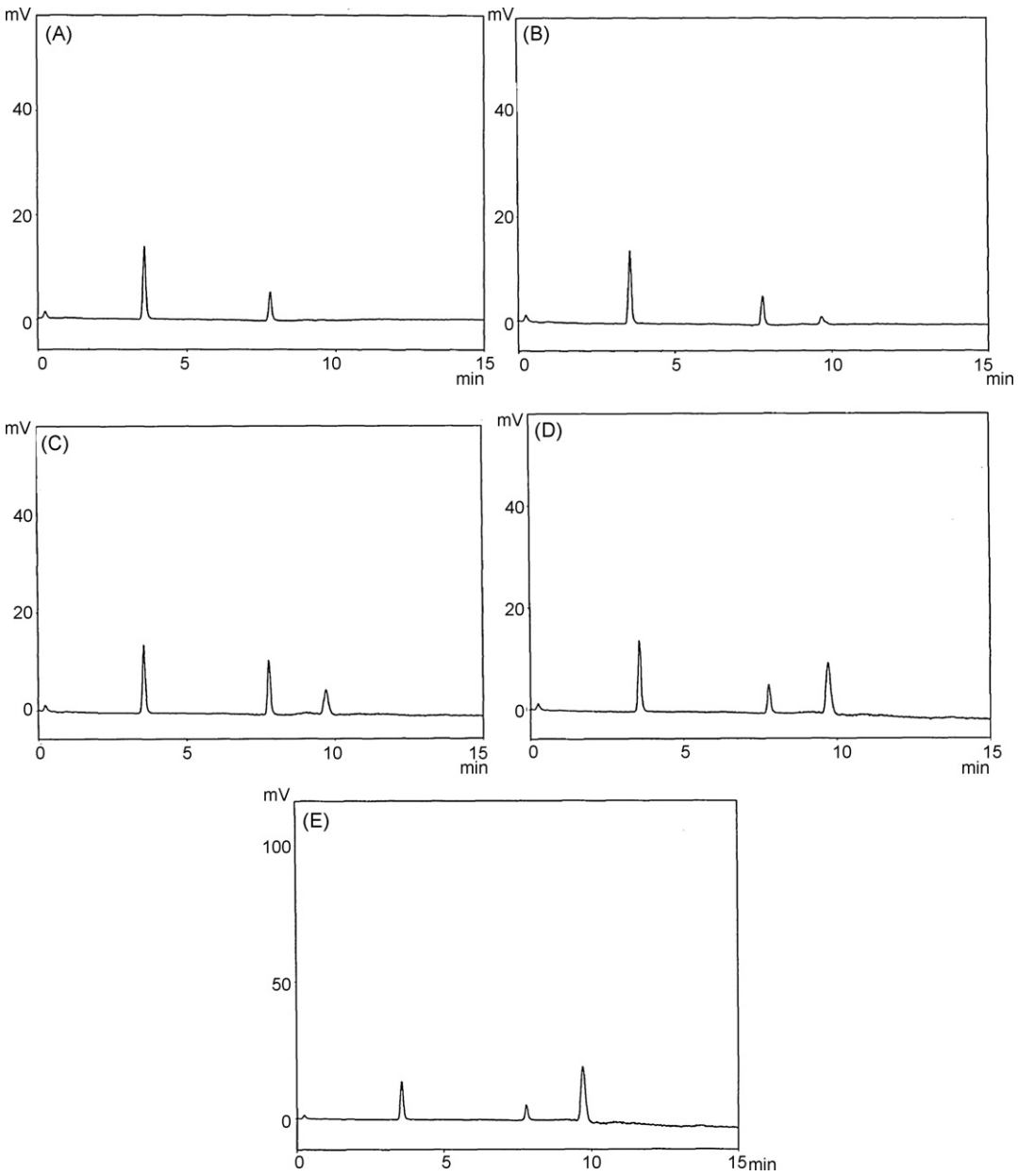

Fig. 7. HPLC spectra of the Suzuki reaction using Pdtnp solution (A) 0 min, (B) 3 min, (C) 6 min, (D) 9 min, and (E) 12 min interval collected samples.

and the binding with CTAB matches with that of Pd–CTAB in Pdnp.

3.6. Surface catalytic activity of trimetallic nanoparticles (Pdtnp) in Suzuki reaction

The similar procedure reported by Mostafa A. El-Sayed et al. was followed in Suzuki coupling reaction the Pd colloidal solution stabilized by polymer [42]. The reaction mixture monitored with HLPC. Fig. 7 shows the HPLC analysis of a sample of the reaction mixture in the first 12 min of reaction. The reaction and the product major peaks are detected, and the peaks with retention times of 3.6, 7.8, and 9.8 min are assigned to phenylboronic acid, iodobenzene, and biphenyl product, respectively, by comparison with standard biphenyl samples. It can be seen clearly from Fig. 7 that the amount of biphenyl is increased with time. At various time intervals the product (biphenyl) formation is conformed using authentic product.

Fig. 7 shows the initial rate of the Suzuki reaction catalyzed by palladium containing trimetallic nanoparticles (Pdtnp). Fig. 7(A) represents each catalytic reaction is carried out three times to examine reproducibility. As can be seen from Fig. 7, the initial reaction rate is increased with increased the product yield.

Fig. 7(A–E) shows the initial rate of the Suzuki reaction catalyzed by palladium containing trimetallic nanoparticles (Pdtnp) and conversion of the biphenyl for the test reaction. The product yields were determined by HPLC analysis. Each spectra shows every 3 min time intervals using 0.5 mol% Pdtnp was sufficient to catalyze the coupling with conversion and product yield of >95%. We have successfully fabricated the first example of an alloy like Au–Ag–Pd trimetallic nanoparticle (Pdtnp) using wet chemical method of mixtures consisting of Au, Ag, and Pd colloids. The present Pdtnp nanoparticles demonstrated good catalytic properties on the C–C coupling reaction, and performing better than a traditional Pd complex catalyst.

Table 1
Reaction conditions, catalysts nature and effects of base, temperature, solvent nature and the product yield of the Suzuki reaction. [Phenylboronic acid] = 1.05 mmol, [iodobenzene] = 1.00 mmol 3:1 molar ratio of DMF–water*.

Entry	Catalyst type	Amount of catalysts (mol%)	Base	Solvent	Reaction temperature (°C)	Product yield (%)[a]
1	Pdnp	0.5	CH_3COONa	DMF–H_2O	100	86.0
2	tnp (1:1:1)	0.5	CH_3COONa	DMF–H_2O	100	99.0
3	tnp (1:1:1)	0.5	NaOH	DMF–H_2O	100	80.0
4	tnp (1:1:1)	0.5	K_2CO_3	DMF–H_2O	100	92.0
5	tnp (1:1:1)	0.5	Et_3N	DMF–H_2O	100	86.0
6	tnp (1:1:1)	0.5	CH_3COONa	DMF	100	94.0
7	tnp (1:1:1)	0.5	CH_3COONa	CH_3CN	100	96.0
8	tnp (1:1:1)	0.5	CH_3COONa	DMF–H_2O	120	96.0
9	tnp (1:1:1)	0.5	CH_3COONa	DMF–H_2O	150	99.0
10	tnp (1:1:1)	0.6	CH_3COONa	DMF–H_2O	100	99.0
11	tnp (1:1:1)	0.4	CH_3COONa	DMF–H_2O	100	94.0
12	tnp (1:1:1)	0.2	CH_3COONa	DMF–H_2O	100	90.0
13	–	–	CH_3COONa	DMF–H_2O	100	36.0

* *Reaction conditions:* Phenylboronic acid (1.05 mmol), iodobenzene (1.00 mmol), CH_3COONa (3.00 mmol), 12 h.
[a] Isolated yield.

3.7. The effects of nature of base, solvent, catalyst and reaction temperature on the Suzuki reaction

The catalytic activity of the Pdnp and Pdtnp towards the Suzuki reaction in the light of quantitative percent yield, reaction time, and recyclability of the catalysts are followed and presented in Table 1. The optimization for the best yield of the product has been carried out by investigating the effects of nature of base, solvent, catalyst and reaction temperature on the Suzuki reaction and the same are presented in Table 1.

The product percentage yields obtained from different reactant compositions show the optimum reactant compositions for maximum yield as those mentioned in the Suzuki reaction procedure (Table 1). The results of product yields given in Table 1 are determined by using the optimum reactant compositions only. The Entries 1 and 2 in Table 1 refer to the inferences obtained from the effects of catalysts nature. Among the metallic nanoparticles system, Pdtnp catalysis shows maximum yield compared to the Pdnp nanoparticles system.

The Entries 2–5 in Table 1 refer to the results of the effect nature of base (3.0 mmol) keeping the reaction temperature (100 °C), solvent (DMF–water 3:1 (v/v) mixture) and 0.5 mol% catalyst as constant parameters. Maximum product yields for both Pdnp and Pdtnp catalysts are found with Sodium acetate as the base and at 100 °C. When Suzuki reaction was carried out with different solvents such as DMF–water and acetonitrile (Table 1, Entries 2, 6 and 7) the product yields are found lesser for the DMF–water 3:1 mixture as the solvent. The temperature effects studies show that, the optimum reaction temperature is found at 100 °C, since 120 and 150 °C reaction temperatures also produced the same percentage yield (Table 1, Entries 2, 8 and 9). In all, 3.0 mmol Sodium acetate incorporated Suzuki reaction, when carried out in DMF–water (3:1) solvent mixture, loaded with 0.5 mol% of the catalyst, at 100 °C produced the maximum percentage yield of the product in the least reaction time (12 h) when the catalyst is Au–Ag–Pd, 1:1:1 Pdtnp. Also, the Pdtnp serve as better catalysts for the Suzuki reaction, since Pdtnp produced higher yields than the corresponding Pdnp catalyst.

The Entries 2, 10–12 in Table 1 refer to the inferences obtained from the effects of catalysts loading to the Suzuki reaction. Among the various concentration of metallic nanoparticles system, Pdtnp with 0.5 and 0.6 mol% catalysis shows maximum yield compared to the other nanoparticles system. This reaction studied without catalysts (Entry 13 in Table 1) gave only 36.0 percentages of the Suzuki products.

3.8. The substitution effects of aryl halide and boronic acid derivatives—Suzuki reaction

All reactions proceeded in 1:1.05 stoichiometric ratios of aryl halide and boronic acid using 3 mmol aqueous sodium acetate as base in exposure to air and trimetallic nanoparticles. The results are summarized in Table 2. The reaction exhibits high efficiency and functional group tolerance. The cross-coupling reaction of iodobenzene (Table 2, Entries 1–3) including a rather electron-rich one (Table 2, Entry 2) with phenylboronic acid proceeded efficiently in metal nanoparticle catalysis and were all complete within 12 h at 120 °C. In addition, bromobenzene exhibited comparable reactivity towards coupling with phenylboronic acid (Table 2, Entry 4). Then the scope of the reaction was expanded by altering the arylboronic acid partner using 4′-bromoacetophenone as aryl halide (Table 2, Entries 5–8). The cross-coupled biaryl products can be furnished in high yields. In particular, aryl chlorides can efficiently react with arylboronic acids under the present condition (Table 2, Entries 9–13). The reaction of chlorobenzene with phenylboronic acid underwent smoothly affording biphenyl with 64% yield in 12 h (Table 2, Entry 9).

3.9. Recovery of trimetallic nanoparticles (tnp) catalysts

The recovery of the catalyst was also investigated. It was found that the palladium containing trimetallic catalysts were fairly stable after the coupling reaction even exposure to air. Then the coupling of phenylboronic acid with Iodobenzene was examined in the presence of 0.5 mol% of tnp to study the recovery of the catalyst and solvent (Table 1). After the completion of the reaction, 0.1 M HCl solution and 3-fold excess of dichloro methane (CH_2Cl_2) are added so that, the trimetallic nanoparticles (Pdtnp) catalyst and the products are correspondingly separated into the pH-responsive aqueous and organic phases, respectively. The precipitate of pH-responsive metallic nanoparticles catalyst was collected by ultracentrifugation. The collected catalyst is dried and reused for the next cycle of reaction. When the recovered catalyst is UV–visible spectra recoated, the spr peaks are not as prominent as in the first cycle. The same reaction mixture solution was used for recycling after the addition of fresh amounts of the reactants. For recycling, an iodobenzene (1 mmol), phenylboronic acid (1.05 mmol) and sodium acetate (3 mmol) were added without addition of any nanoparticle. The reaction mixture was then refluxed for another 12 h to complete the second cycle.

Table 2
Trimetallic nanoparticles (tnp) mediated Suzuki cross-coupling reaction of aryl halides with boronic acids.

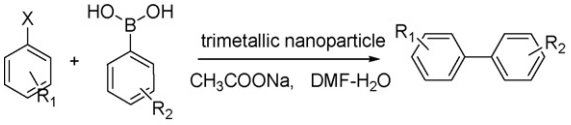

X = Cl, Br, I
R_1 = H, CH_3, OCH_3, $COCH_3$, NO_2
R_2 = H, CH_3, OCH_3

R_1 = H, CH_3, OCH_3, $COCH_3$, NO_2
R_2 = H, CH_3, OCH_3

Entry	R^1	X	R^2	Reaction time (h)	Isolated yield (%)[a]
1	H	I	H	12	99, 94[b]
2	4-OCH_3	I	H	12	80
3	3,5-$(CH_3)_2$	I	H	12	86
4	H	Br	H	12	94
5	4-Ac	Br	H	12	96
6	4-Ac	Br	4-CH_3	12	90
7	4-Ac	Br	4-OCH_3	12	92
8	4-Ac	Br	3,5$(CH_3)_2$	12	94
9	H	Cl	H	12	64
10	4-Ac	Cl	H	12	76
11	4-Ac	Cl	4- CH_3	12	72
12	4-Ac	Cl	3,5-$(CH_3)_2$	12	78
13	4-NO_2	Cl	H	12	74

[*] *Reaction conditions:* Phenylboronic acid (1.05 mmol), iodobenzene (1.00 mmol), CH_3COONa (3.00 mmol), and trimetallic catalyst (0.5 mol%), DMF–H_2O (3:1).
[a] Isolated yield.
[b] Yield after 2nd cycle.

As clearly shown in Fig. 7, the trimetallic nanoparticle showed much better catalytic activity than monometallic nanoparticle, which resulted from the larger number of nanoparticles derived from the core/shell structure (an equal amount of nanoparticle was used). The nanoparticle catalyst can be recycled and reused at least three times without losing the catalytic activity. We have successfully fabricated the first example of an Au–Ag–Pd trimetallic nanoparticle using wet chemical method of mixtures consisting of Au, Ag, and Pd colloids. Fig. 7 shows that the present Au–Ag–Pd trimetallic nanoparticles demonstrated good catalytic properties on the product formation test platform, performing better than a traditional Pd containing monometallic catalyst.

4. Conclusions

Temperature controlled preparation of Au–Ag–Pd trimetallic nanoparticles with Au-core/Ag-interlayer/Pd-shell structure using CTAB as the capping agent has been reported. Surface plasmon peaks in UV–vis spectroscopy has been used to monitor the sequential deposition of mono-, bi- and trimetallic nanoparticles at the different temperature regions. FT-IR spectra conformed the UV–visible inferences. The HRTEM photographs of Pdnp, Au–Ag and Pdtnp showed the sizes as 6.0 ± 0.5, 9.0 ± 0.5 and 13.0 ± 0.5 nm, respectively. The particle size results from TEM and XRD agree well with each other. Pdtnp catalysis of Suzuki reaction produced better results than Pdnp catalysts. Infact, presence of metal nanoparticles as catalysts replaces enviro-deadlier catalytic strong bases being used in Suzuki reaction. Metal nanoparticles as catalysts also yielded appreciably high yield of the product, biphenyl. The high catalytic activity of trimetallic nanoparticles is probably due to the sequential electronic effect between elements in a particle. The preparation and characterization techniques presented here will be useful to design novel catalysts with desired structure.

Acknowledgments

The author thank to I.I.T. Madras, India for recording TEM of samples recovered from different stage of preparations. Financial support to the Department from DST-FIST is also acknowledged.

References

[1] H. Bonnemann, R.M. Richards, Eur. J. Inorg. Chem. (2001) 2455.
[2] G. Schmid (Ed.), Clusters and Colloids from Theory to Application, VCH, Weinheim, 1994.
[3] H. Hirai, N. Toshima, in: Y. Iwasawa (Ed.), Tailored Metal Catalyst, Reidel, Dordrecht, 1985, p. 121.
[4] H. Bonnemann, W. Brijoux, R. Brinkmann, E. Dinjus, T. Jouben, B. Korall, Angew. Chem., Int. Ed. Engl. 30 (1991) 1312.
[5] C. Amiens, D. de Caro, B. Chaudret, J.S. Bradley, R. Mazel, C. Roucau, J. Am. Chem. Soc. 115 (1993) 11638.
[6] N. Toshima, Y. Shiraishi, T. Teranishi, M. Miyake, T. Tominaga, H. Watanabe, W. Brijoux, H. Bonnemann, G. Schmid, Appl. Organomet. Chem. 15 (2001) 178.
[7] H. Tsunoyama, H. Sakurai, Y. Negishi, T. Tsukuda, J. Am. Chem. Soc. 127 (2005) 9374.
[8] S. Sun, C.B. Murray, D. Weller, L. Folk, A. Moser, Science 287 (2000) 1989.
[9] M. Chen, J. Kim, J.P. Liu, H. Fan, S. Sun, J. Am. Chem. Soc. 128 (2006) 7132.
[10] M. Nakaya, M. Kanehara, T. Teranishi, Langmuir 22 (2006) 3485.
[11] X. Du, N. Toshima, Chem. Lett. 35 (2006) 1254.
[12] N. Watanabe, N. Toshima, Bull. Chem. Soc. Jpn. 80 (2007) 208.
[13] S. Kobayashi, T. Miyama, N. Nishida, Y. Sakai, H. Shiraki, Y. Shiraishi, N. Toshima, J. Disper. Sci. Technol. 2 (2006) 121.
[14] H. Iida, T. Nakanishi, T. Osaka, Electrochim. Acta 51 (2005) 855.
[15] J.S. Bradley, in: G. Schmid (Ed.), Clusters and Colloids: From Theory to Applications, VCH, Weinheim, 1994, p. 523.
[16] N. Toshima, T. Yonezawa, New J. Chem. 22 (1998) 1179.
[17] M.B. Thathagar, J. Beckers, G. Rothenberg, J. Am. Chem. Soc. 124 (2002) 11858.
[18] D. Brinzei, L. Catala, C. Mathonie re, W. Wernsdorfer, A. Gloter, O. Stephan, T. Mallah, J. Am. Chem. Soc. 129 (2007) 3778.
[19] R.G. Haverkamp, A.T. Marshall, D. van, Agterveld, J. Nanoparticle Res. 9 (2007) 697.
[20] N. Toshima, R. Ito, T. Matsushita, Y. Shiraishi, Catal. Today 122 (2007) 239.
[21] B. Schmor, R. Roy, Molecules 7 (2002) 433.
[22] R.K. Arvela, N.E. Leadbeater, J. Org. Chem. 70 (2005) 1786.
[23] J.G. de Vries, Dalton Trans. (2006) 421.
[24] I. Ozdemir, Y. Gok, N. Gurbuz, B. Cetinkaya, Turk. J. Chem. 31 (2007) 397.
[25] L. Strimbu, J. Liu, A.E. Kaifer, Langmuir 19 (2003) 483.
[26] Y. Li, X.M. Hong, D.M. Collard, M.A. El-Sayed, Org. Lett. 15 (2000) 2385.
[27] R. Rajagopal, D.V. Jarikote, K.V. Srinivasan, Chem. Commun. (2002) 616.
[28] Y. Li, M.A. El-Sayed, J. Phys. Chem. B 105 (2001) 8938.
[29] S. Kidambi, J. Dai, J. Li, M.L. Bruening, J. Am. Chem. Soc. 126 (2004) 2658.
[30] Z. Kiraly, B. Veisz, A.A. Mastalir, G. Kofarago, Langmuir 17 (2001) 5381.
[31] S.J. Kim, S.D. Oh, S. Lee, S.H. Choi, J. Ind. Eng. Chem. 14 (2008) 449.
[32] B. Pergolese, M.M. Miranda, A. Bigotto, Chem. Phys. Lett. 438 (2007) 290.
[33] W. Hou, N.A. Dehm, R.W.J. Scott, J. Catal. 253 (2008) 22.
[34] P. Dash, N.A. Dehm, R.W.J. Scott, J. Mol. Catal. A: Chem. 286 (2008) 114.
[35] J. Kugai, V. Subramani, C. Song, M.H. Engelhard, Y.-H. Chin, J. Catal. 238 (2006) 430.

[36] S.H. Tsai, Y.H. Liu, P.L. Wu, C.S. Yeh, J. Mater. Chem. 13 (2003) 978.
[37] A.V. Singh, B.M. Bandgar, M. Kasture, B.L.V. Prasad, M. Sastry, J. Mater. Chem. 15 (2005) 5115.
[38] H. Tan, T. Zhan, W.Y. Fan, Chem. Phys. Lett. 20 (2006) 352.
[39] S. Bharathi, N. Fishelson, O. Lev, Langmuir 15 (1999) 1929.
[40] L.G. Sillen, A.E. Martell, Stability Constants of Metal-Ion Complexes, Special Publication No. 17, the Chemical Society, London, 1964.
[41] R.M. Smith, A.E. Martell, Critical Stability Constants: Amines, vol. 2, Plenum, New York, 1975.
[42] Y. Li, E. Boone, M.A. El-Sayed, Langmuir 18 (2002) 4921.